Microstructure, Wettability, and Thermal Stability of Semifluorinated Self-Assembled Monolayers (SAMs) on Gold

H. Fukushima,* S. Seki, T. Nishikawa, and H. Takiguchi

Base Technology Research Centre, Seiko Epson Co. 3-3-5, Owa, Suwa, Nagano-ken, 392-8502, Japan

K. Tamada and K. Abe

NIMC, 1-1 Higashi, Tsukuba, Ibaraki-ken, 305-8565, Japan

R. Colorado, Jr., M. Graupe, O. E. Shmakova, and T. R. Lee

Department of Chemistry, University of Houston, Houston, Texas 77204-5641

Received: January 28, 2000; In Final Form: May 15, 2000

The microstructure, wettability, and thermal stability of self-assembled monolayers (SAMs) on gold generated from semifluorinated alkanethiols $F(CF_2)_{10}(CH_2)_nSH$, where $n = 2$, 6, 11, 17, and 33 (F10H*n*SH), were examined by polarization modulation infrared reflection absoprtion spectroscopy (PM-IRRAS) and dynamic contact angle measurements. Analysis by PM-IRRAS revealed that the length of the methylene spacer (Hn) influenced the tilt angle of the fluorocarbon segments in the semifluorinated SAMs. As the length of the methylene spacer was increased, the tilt angle of the perfluorocarbon moiety increased with respect to the surface normal. The longer methylene spacers (H*n*, $n = 11$, 17, and 33) exhibited well-ordered trans-extended conformations as indicated by the position of the antisymmetric methylene band ($\nu_a^{CH_2} = 2919$ cm^{-1}). Shortening the length of the methylene spacer to $n = 6$, however, led to a decrease in conformational order ($\nu_a^{CH_2} = 2925$ cm^{-1}). Dynamic contact angle measurements using the Wilhelmy plate method showed that the semifluorinated SAMs were poorly wet by both water (average $\theta_a = 120°$) and hexadecane (average $\theta_a = 81°$). The wettability varied with the length of the methylene spacer; in particular, both the thinnest and the thickest semifluorinated SAMs (derived from F10H2SH and F10H33SH, respectively) exhibited relatively low dynamic contact angle values. In addition, the thermal stability of the semifluorinated SAMs was found to increase as the length of the methylene spacer was increased. Overall, these films exhibited remarkable resistance to thermal degradation (e.g., SAMs derived from F10H33SH sustained a relatively high contact angles after incubation at 150 °C for 1 h in air).

Introduction

Self-assembled monolayers (SAMs) generated from alkanethiol derivatives with specifically functionalized tail groups have been studied intensively during the past decade.[1] Many of these studies have been directed toward the development of microengineering tools for industrial applications such as biomedical devices,[2] optical devices,[3] liquid crystals,[4] and microlithography[5] and as models of surface lubricants in microtribology.[6] A significant obstacle to the implementation of SAMs in everyday applications is the poor durability of these thin films under ambient and more extreme conditions. For example, SAMs of alkanethiols on gold begin to lose their ordered monolayer structure and decompose at temperatures over 100 °C.[7] Strategies employed to prevent the deterioration of SAMs on gold have included the incorporation of laterally polymerized conjugated alkyne moieties in the alkanethiols,[8] the introduction of three-dimensional multiple hydrogen bond networks derived from amide groups in the alkanethiols,[9] and the use of underpotentially deposited metal layers of Cu or Ag on gold surfaces used as substrates for SAM growth.[10]

The introduction of fluorocarbon chains as terminal groups in alkanethiol molecules is also expected to enhance the durability of SAMs. Fluorocarbon terminal groups have been studied in comparison with other functional groups such as −OH, −COOH, and $-CH_3$ to evaluate the influence of terminal group chemical nature on the surface properties.[1d,11] In these studies, the SAMs generated from the semifluorinated alkanethiols were robust and relatively defect-free. Perfluorocarbon chains adopt a helical conformation and consequently possess larger cross sections than those of hydrocarbon chains (e.g., the van der Waals diameter of a fluorocarbon chain is 5.6 Å whereas that of a hydrocarbon chain is 4.2 Å).[1d,11] Furthermore, perfluorocarbon chains are more rigid than analogous hydrocarbon chains,[12] and they are more resistant to oxidation and corrosion.[13] These factors all contribute to the enhanced stability of fluorocarbon-containing materials against mechanical friction, thermal stress, and extreme acid/base conditions.

A number of structural studies on SAMs derived from semifluorinated alkanethiol derivatives such as $F(CF_2)_m(CH_2)_n$-SH ($m = 6$, 8, 12; $n = 2$)[1d,11,12] ($m = 8$; $n = 11$)[14] and $F(CF_2)_m$-$CONH(CH_2)_2SH$ ($m = 7$, 8, 9)[15] have been performed. Moreover, SAMs derived from semifluorinated disulfides have been used to probe the mechanism(s) of phase separation of mixed monolayer systems on gold.[16] Tamada et al.[17] also studied the tilt angle of perfluorocarbon segments in two semifluorinated

* Corresponding author. E-mail: fukushima.hitoshi@exc.epson.co.jp.

10.1021/jp0003499 CCC: $19.00
Published on Web 07/18/2000

alkanethiol monolayers on gold (F8H6SH and F10H11SH) as a function of the length of the methylene spacer. These studies indicated that the length of the methylene spacer influenced the orientation of the terminal perfluorocarbon segments.

Despite these efforts, there has been no systematic investigation of the role of the methylene spacer in semifluorinated alkanethiol SAMs in determining the properties of these films. In particular, such an investigation would address the following issues: (1) What is the influence of the methylene spacer on the microstructure of the SAMs? An understanding of the interplay between the length of the methylene spacer and the resultant microstructure of SAMs should provide crucial insights into the design of useful fluorinated materials. (2) What is the influence of the methylene spacer on the surface properties, such as the wettability, of SAMs? Understanding this relationship would permit the fabrication of fluorinated coatings with controlled surface properties. (3) What is the influence of the methylene spacers on the durability of the SAMs against thermal stress,[7a] mechanical friction, and other environmental strains? The latter issue is particularly relevant to the use of fluorinated SAMs in industrial applications.

In this report, we examine the influence of the length of the methylene spacer upon the microstructure, wettability, and thermal stability of SAMs on gold generated from a series of semifluorinated alkanethiol derivatives, $F(CF_2)_{10}(CH_2)_nSH$, where $n = 2$, 6, 11, 17, and 33 (F10H*n*SH). PM-IRRAS was used to probe the tilt of the perfluorocarbon segement and the conformational order of the methylene spacer. Dynamic contact angle measurements were used to determine the wettability of these films toward water and hexadecane and to monitor the thermal stability of these films under ambient conditions.

Experimental Section

Synthesis of Semifluorinated Alkanethiols. F8H6SH was purchased from Dojindo Laboratory (Kumamoto, Japan). The rest of semifluorinated alkanethiols were synthesized using methodologies described in a previous report.[18] Complete analytical data for all new compounds will be provided separately.[19]

Gold Substrate and Monolayer Preparation. The Au(111)/mica substrates were prepared by the epitaxial growth of a gold film (100−150 nm thick) onto freshly cleaved mica in a vacuum chamber (Biemtron Co. Ltd., Mito, Japan). Prior to evaporation, the mica surface was annealed at 550 °C for 3 h at a pressure between 10^{-7} and 10^{-8} Torr. The evaporative deposition of gold was then conducted at a rate of 0.1 nm/s as the substrate temperature was maintained at 350 °C. After the gold was deposited, the substrate was again annealed at 550 °C for 1.5 h. This procedure afforded an atomically flat Au(111) surface with crystal grains measuring 50−100 nm in diameter. The Au(111) substrates were removed from the vacuum chamber and immersed into freshly prepared semifluorinated alkanethiol solutions (0.2 mM in dichloromethane) within 10 min after exposure to air. The substrates were left in each solution for 1 day and were then washed in pure warm dichloromethane for 30 min. Finally, the substrates were dried under nitrogen and immediately characterized.

For the PM-IRRAS experiments, the gold substrates (∼1 cm × 3 cm) were prepared by thermally evaporating a thin layer of chromium (∼100 Å) onto the polished surface of a silicon wafer and then thermally evaporating gold (∼2000 Å). The semifluorinated alkanethiols were adsorbed onto these Au/Cr/Si substrates using the procedure described in the preceding paragraph.

Dynamic Contact Angle Measurements. Dynamic contact angle measurements were performed using the Wilhelmy plate method with a Cahn balance (DCA 322 model). The Wilhelmy plate method enables highly accurate measurements on wide surfaces (cm range) without interpretive errors of the sort encountered using contact angle goniometry. Fine control of both advancing and receding speeds was achieved through the use of a dc motor drive. A modified technique was used to measure dynamic contact angles on one-sided Au−thiol SAM plates (surface, Au−thiol SAMs; back, cleaved mica; substrate size, 1 cm × 2 cm × 50 μm). All measurements utilized pure water and HPLC grade hexadecane at advancing and receding speeds of 20 μm/s. Exact details of this technique were presented in a previous report.[20] All measurements were performed at room temperature (22 ± 1 °C) in a clean room.

Infrared Spectroscopy. Fourier transform infrared (FTIR) spectra of the bulk semifluorinated alkanethiols were measured using a Magna 560 Fourier transform spectrometer (Nicolet) in diffuse reflectance mode. The bulk samples were mixed homogeneously with KBr, and each spectrum was taken by collecting 200 scans at a resolution of 4 cm^{-1} over the 4000−600 cm^{-1} spectral region.

Polarization modulation infrared reflection absorption infrared spectroscopy (PM-IRRAS) data were collected using a Magna 860 Fourier transform spectrometer (Nicolet) equipped with a liquid-nitrogen-cooled mercury−cadmium−telluride (MCT) detector and a PEM-90 photoelastic modulator (Hinds Instruments). The infrared light was modulated between s- and p-polarizations at a frequency of 37 kHz and was incident upon the sample surface at 80°. Signals generated from each polarization (R_s and R_p) were detected simultaneously by a lock-in amplifier and used to calculate the differential surface reflectivity $(\Delta R/R) = (R_p - R_s)/(R_p + R_s)$. The spectra were taken by collecting 500 scans at a spectral resolution of 4 cm^{-1}.

Evaluation of Thermal Stability. Gold films with a thickness of 1000 Å were sputtered onto titanium-primed (100 Å) quartz substrates (20 mm × 50 mm × 1.0 mm). Each freshly prepared substrate was immersed into a semifluorinated alkanethiol solution for 12 h. After immersion, each substrate was washed with pure warm dichloromethane to thoroughly remove any physisorbed species. Each substrate was then dried and left under nitrogen until the experiments were performed.

Initial contact angles of the SAMs were determined by the sessile drop method using hexadecane as the probe liquid. The sessile values were reproducibly lower by 10 ± 2° than those obtained by the dynamic contact angle method described above except for SAMs derived from F10H33SH; the sessile values on these SAMs were lower by 4 ± 2° than those obtained using the dynamic contact angle method. This discrepancy might arise from differences in the fabrication of the Au substrates (e.g., differences in surface roughness or the presence of contaminants) or perhaps differences inherent to the two analytical methods. While these differences might influence absolute measurements of thermal stability, relative comparisons of the contact angle data should, nevertheless, provide meaningful trends in stability within a given series of SAMs. The semifluorinated SAMs were heated in air inside a temperature-controlled oven system. After 1 h of incubation, each substrate was washed with dichloromethane and subjected to analysis by contact angle goniometry. The resulting data were averaged over 5 random measurements on a given surface.

Results and Discussion

1. Infrared Spectroscopy. Two regions of the IR spectrum contain bands that are characteristic of semifluorinated al-

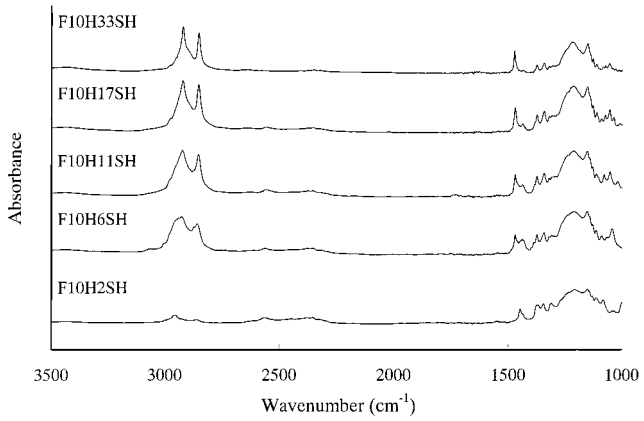

Figure 1. FTIR spectra of semifluorinated alkanethiols, F10H*n*SH (n = 2, 6, 11, 17, and 33) in the bulk state. The measurements were conducted in diffuse reflection mode.

kanethiols. One is the C−F stretching region ranging from 800 to 1500 cm^{-1}, and the other is the C−H stretching region ranging from 2800 to 3000 cm^{-1}.[11,21] To identify the characteristic bands of semifluorinated alkanethiol monolayers on gold, we first analyzed the IR spectrum of each bulk sample (Figure 1). The bands in the range from 1100 to 1300 cm^{-1} were assigned to overlapping antisymmetric ($\nu_{as}^{CF_2}$) stretching, symmetric ($\nu_{s}^{CF_2}$) stretching, C−C (ν^{CC}) stretching, and CCC (δ^{CCC}) bending using assignments from past studies of fluorocarbon materials.[22] The CF_2 stretching modes dominate this region and possess transition dipole moments that are perpendicular to the fluorocarbon helical axis. For simplicity, we will refer to these bands collectively as perpendicular CF_2 stretching bands ($\nu_{pd}^{CF_2}$). In contrast, the two bands at 1340 and ∼1370 cm^{-1} possess transition dipole moments that are parallel to the fluorocarbon axis and are commonly referred to as axial CF_2 stretching vibrations ($\nu_{ax}^{CF_2}$).[11,14] If one assumes that the intensities of $\nu_{pd}^{CF_2}$ are amplified with respect to the intensities of $\nu_{ax}^{CF_2}$ when the helical fluorocarbon chains are oriented parallel to the Au surface, these orthogonal modes provide convenient orientational information regarding the perfluorocarbon segments of semifluorinated SAMs.[15] Accordingly, the intensities of $\nu_{pd}^{CF_2}$ diminish with respect to the intensities of $\nu_{ax}^{CF_2}$ when the perfluorocarbon segments are oriented perpendicular to the Au surface. On the basis of these assumptions, we were able to monitor the relative tilt of the perfluorocarbon segment as the length of the methylene spacer in the semifluorinated SAMs was increased. As the series progressed from F10H2SH to F10H33SH, the intensity of $\nu_{pd}^{CF_2}$ increased with respect to the intensity of $\nu_{ax}^{CF_2}$ (Figure 2). We therefore conclude that the perfluorocarbon moiety tilts progressively more from the surface normal as the length of methylene spacer increases through this series of SAMs.

SAMs derived from *n*-alkanethiols exhibit characteristic C−H stretching bands attributable to both methylene and methyl groups.[23] Since, however, SAMs derived from fluorocarbon-terminated alkanethiols contain no methyl groups, their spectra consist of only C−H stretching bands arising from the methylene groups (vide infra). Although the absence of CH_3 moieties precludes a rigorous IR-based evaluation of the tilt angle of the hydrocarbon segment, it is possible to qualitatively evaluate the conformational order of the methylene spacer in semifluorinated SAMs by examining the $\nu_{a}^{CH_2}$ band position and width.[14,23,24] According to previous IR studies of the hydrocarbon chains of SAMs, the position of the $\nu_{a}^{CH_2}$ band approaches 2918−2919 cm^{-1} when the conformational order of the methylene backbones is predominantly trans extended.[23] This

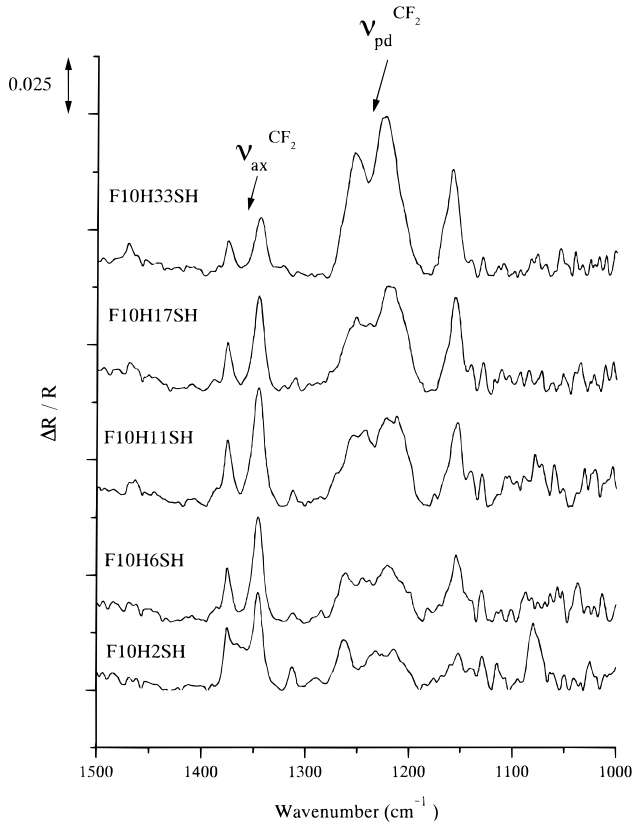

Figure 2. PM-IRRAS spectra of SAMs generated from F10H*n*SH (n = 2, 6, 11, 17, and 33) on gold. The bands between 1100 and 1250 cm^{-1} are assigned to overlapping perpendicular perfluoromethylene stretches ($\nu_{pd}^{CF_2}$). The two bands between 1300 and 1400 cm^{-1} (∼1340 and ∼1370 cm^{-1}) are assigned to axial perfluoromethylene stretches ($\nu_{ax}^{CF_2}$).

characteristic band position is commonly observed for SAMs containing long-chain ($H(CH_2)_nSH$; $n > 10$) crystalline hydrocarbon segments. At shorter *n*-alkanethiol chain lengths, the SAMs become less ordered and more liquidlike;[23] correspondingly, the $\nu_{a}^{CH_2}$ band appears at higher frequencies (e.g., 2924−2926 cm^{-1}), indicating that the methylene groups possess random (e.g., gauche) conformations.

Figure 3 shows the C−H stretching region for the semifluorinated SAMs. The SAMs derived from F10H11SH, F10H17SH, and F10H33SH, which possess relatively long methylene spacers, exhibited $\nu_{a}^{CH_2}$ bands at ∼2919 cm^{-1}, indicating predominantly trans-extended conformations for the hydrocarbon segments. In contrast, the $\nu_{a}^{CH_2}$ band for the SAM derived from F10H6SH appeared as a broad peak between 2920 and 2930 cm^{-1}, suggesting a disordered conformation for the hydrocarbon segment of this SAM.[14,23,24] Since F10H2SH has only two methylene groups, we were unable to detect the $\nu_{a}^{CH_2}$ band for the SAM derived from this adsorbate. Since the strength of stabilizing interchain interactions depends on the number of methylene units in the segments,[25a] the disordered conformation for the F10H6SH SAM probably arises from weak lateral interactions due to the short length of the methylene spacer. This effect is analogous to that previously described for *n*-alkanethiol SAMs, where adsorbates with less than 10 methylene units form progressively disordered films. [23,25a]

2. Dynamic Contact Angles. The wettabilities of SAMs generated from the semifluorinated alkanethiols were determined by dynamic contact angle measurements, which directly reflect the composition and structure of the surfaces probed.[25] Furthermore, because the advancing angle (θ_a) and the receding

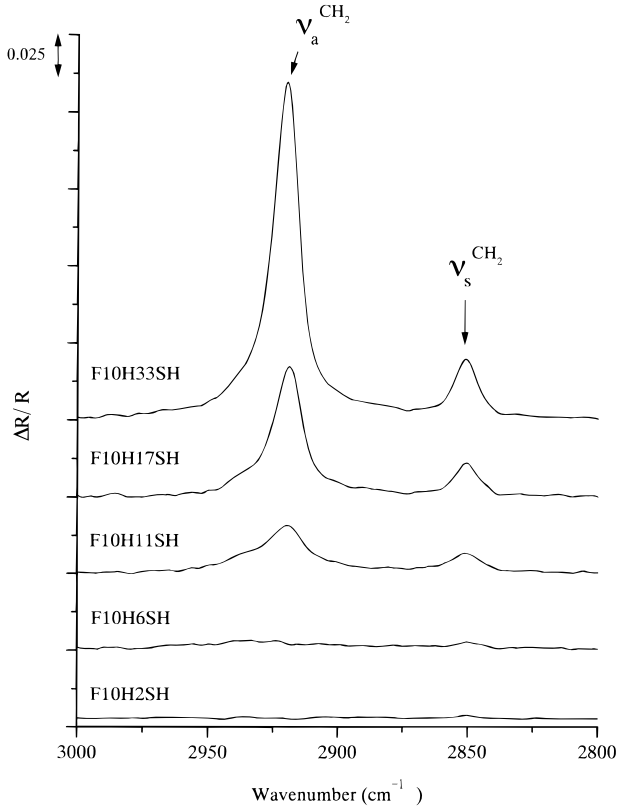

Figure 3. PM-IRRAS spectra of SAMs generated from F10H*n*SH (n = 2, 6, 11, 17, and 33) on gold. The antisymmetric methylene ($\nu_a^{CH_2}$) and symmetric methylene ($\nu_s^{CH_2}$) bands, which appear at 2920 and 2850 cm^{-1}, respectively, are shown. There are no observable corresponding bands for F10H2SH due to the small number of methylenes.

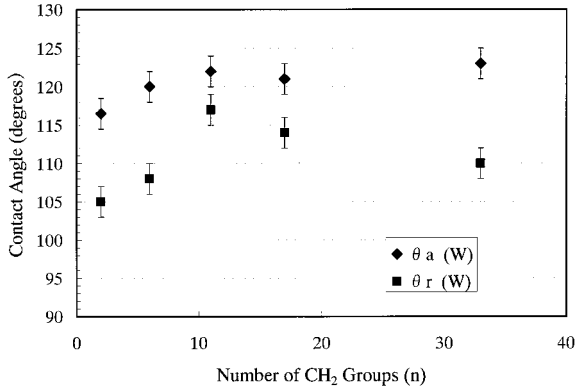

Figure 4. Measurements of the dynamic contact angle of water on SAMs generated from F10H*n*SH (n = 2, 6, 11, 17, and 33) on Au(111) (◆ = advancing angle, θ_a; ■ = receding angle, θ_r).

angle (θ_r) represent two metastable equilibrium states of a contacting liquid on low-energy and high-energy regions, respectively, of a microscopically inhomogeneous surface, the hysteresis between the advancing and receding angle ($\Delta(\cos\theta) = \cos\theta_a - \cos\theta_r$) provides a measure of the degree of surface roughness or heterogeneity of the interface.[25a] The measurements of dynamic contact angle using water and hexadecane are shown in Figures 4 and 5, respectively, and are summarized with their respective hystereses in Table 1. In general, the average advancing contact angles for water ($\theta_a = 120°$) and hexadecane ($\theta_a = 81°$) suggest that the surfaces of semifluorinated SAMs are both highly hydrophobic and highly oleophobic, respectively. Moreover, the average hystereses fall within the range commonly observed for SAMs on Au.[26] The measured contact angle values are consistent with a predominant exposure of CF_3-

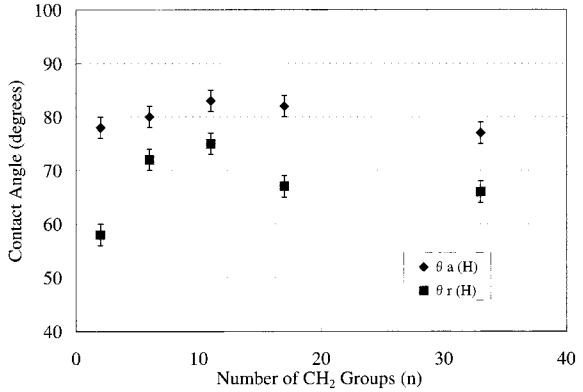

Figure 5. Measurements of the dynamic contact angle of hexadecane on SAMs generated from F10HnSH (n = 2, 6, 11, 17, and 33) on Au(111) (◆ = advancing angle, θ_a; ■ = receding angle, θ_r).

TABLE 1: Dynamic Advancing (θ_a) and Receding (θ_r) Contact Angles (deg) and Hystereses ($\Delta\theta$) (deg)[a]

adsorbate	θ_a(H)	θ_r(H)	$\Delta\theta$(H)	θ_a(W)	θ_r(W)	$\Delta\theta$(W)
F10H2SH	78	58	20	116	105	11
F10H6SH	80	72	8	120	108	12
F10H11SH	83	75	8	122	117	5
F10H17SH	82	67	15	121	114	7
F10H33SH	77	66	11	123	110	13

[a] The notations (H) and (W) correspond to hexadecane and water, respectively. All contact angle values were reproducible within ±2°.

terminated perfluorocarbon moieties at the surface of a densely packed, defect-free film.[27] Analysis of the contact angle data of SAMs derived from specific F10HnSH species, however, suggests some dependence on the length of the methylene spacer.

All of the semifluorinated SAMs exhibit high contact angles of hexadecane, which arise from the weak and nonideal dispersive interactions between hydrocarbons and fluorocarbons.[28] Nevertheless, the contact angles of SAMs derived from F10H2SH (θ_a = 78°) and F10H33SH (θ_a = 77°) were consistently lower than those of the other films ($\theta_a \approx 82°$). In an attempt to rationalize these differences, we considered whether surface microstructure might influence the wettabilities of these chemically equivalent SAM surfaces. Lateral force images obtained by atomic force microscopy (AFM) revealed that the quality of the images became worse, and the ability to obtain images became more difficult as the length of the methylene spacer increased.[29] The SAM derived from F10H2SH was readily imaged and exhibited a highly ordered hexagonal lattice, while the SAM derived from F10H33SH produced only low-resolution images containing periodic striped features. When coupled with the conclusions drawn from the PM-IRRAS data (vide supra), these observations suggest that the two-dimensional surface order of the films degrades when the tilt of the perfluorocarbon segments increases. Moreover, it is possible that the low contact angle of hexadecane observed for the F10H33SH SAM might arise from its relatively disordered surface microstructure.

In contrast, the enhanced wettability of SAMs derived from F10H2SH probably arises from a different phenomenon since this SAM exhibits a highly ordered surface microstructure.[29] Furthermore, the relatively large hysteresis for the F10H2SH SAM probably also arises from a phenomenon other than microscopic surface roughness, since the hysteresis for the F10H33SH SAM, which appears to be disordered at the

nanoscale level (vide supra), is small. Since F10H2SH possesses a thickness that is considerably lower than that of the other films, van der Waals (vdW) interactions between the underlying gold substrate and the contacting liquid above the monolayer might be of sufficient strength to reduce the contact angle. Using Lifshitz theory, Miller and Abbott examined the influence of the underlying gold substrate on the hexadecane contact angles of SAMs of *n*-alkanethiols $H(CH_2)_nSH$ ($n = 3-18$) as a function of film thickness.[30] Both theory and experiment demonstrated that the increased wettabilities of films formed from *n*-alkanethiols of shorter chain length ($n < 10$) were due to vdW interactions with the underlying substrate.

Analysis of the contact angles of water provide additional support for the involvement of substrate-based vdW interactions in the wettability of SAMs derived from F10H2SH. Since water is highly cohesive, it is less sensitive than hexadecane in probing the surface microstructure of nonpolar surfaces by contact angle measurements. Therefore, the observation that water consistently wets the surface of F10H2SH SAMs ($\theta_a = 116°$) more than that of the other SAMs ($\theta_a = 122°$) might be unrelated to changes in surface microstructure. We note that Miller and Abbott proposed that vdW interactions with the underlying substrate should also influence the contact angles of polar liquids.[30] Furthermore, if the lower contact angle of water on F10H2SH were to arise from microstructural surface disorder, a lower contact angle of water would also be expected for the significantly disordered surface of F10H33SH—a result contrary to our observations. Our model requires that substrate-based vdW interactions for the F10H2SH SAM occur through a thicker film (12 carbon atoms) than that proposed Miller and Abbott (10 carbon atoms maximum), which might be reasonable in light of the different dielectric properties (e.g., refractive index, dielectric susceptibilities) of semifluorinated alkanethiol chains vs *n*-alkanethiol chains.

The influence of lateral vdW interactions within the SAMs should also be considered. Lateral forces influence the stability of densely packed semifluorinated SAMs via at least three mechanisms: (1) stabilizing vdW interactions between the perfluorocarbon moieties;[31] (2) stabilizing vdW interactions between the methylene moieties;[31] (3) destabilizing (repulsive) dipole−dipole interactions arising from the junction between the perfluorocarbon and methylene moieties.[32] These combined factors influence the structure of SAMs generated from F10HnSH and their corresponding cohesive interaction against contacting liquids. Experiments and simulated calculations to further explore the effect of these phenomena on semifluorinated SAMs are currently underway.

We also note that evaluation of the microstructure of fluorinated films using hydrocarbon contacting liquids can be complicated by both the nonideal interactions between fluorocarbons and hydrocarbons and the relative molecular sizes of the contacting liquids.[28]

3. Thermal Stability. Given that future applications involving semifluorinated SAMs might require stability over a range of temperatures in the ambient atmosphere, we evaluated the thermal stability of these films in air. The deterioration of alkanethiol SAMs on gold under thermal stress has been reported.[7a,25a,33] Because the loss of film order leads to an enhanced wettability of the SAM surface, we used hexadecane contact angle measurements to monitor surface disordering and film degradation as a function of incubation temperature (Figure 6). For all monolayers examined, the contact angles decreased as the incubation temperature increased. At each incubation temperature, however, the extent of this contact angle decrease

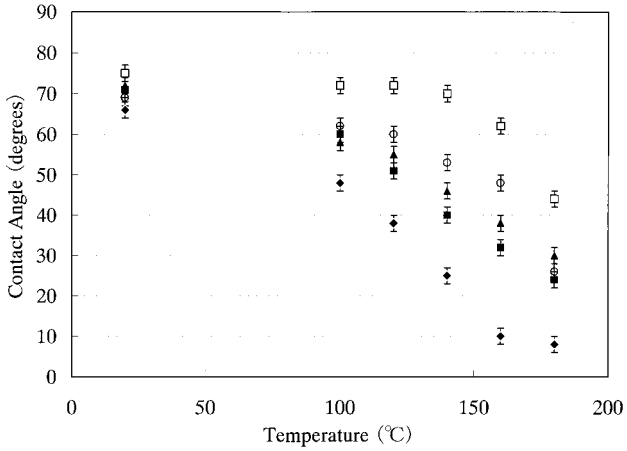

Figure 6. Plot of advancing contact angle vs incubation temperature. SAMs were generated from F10HnSH ($n = 2$, 6, 11, 17, and 33) on Au/Ti/quartz substrates (◆ = F10H2SH; ■ = F10H6SH; ▲ = F10H11SH; ○ = F10H17SH; □ = F10H33SH).

was greater in SAMs with shorter methylene spacers. This effect was readily observed at incubation temperatures above 150 °C, where each successively shorter chain length exhibited a successively lower contact angle (and thus a successively higher wettability). After the final incubation at 180 °C, the contact angle on the F10H33SH SAM had decreased from 75 to 43° (43% decrease), the contact angle on the F10H17SH, F10H11SH, and F10H6SH SAMs had decreased from ∼70 to 25° (64% decrease), and the contact angle on the F10H2SH SAM had decreased from 63 to 8° (87% decrease). The superior durability of films that contain longer methylene moieties likely originates from differences in the strength of the lateral intermolecular van der Waals interactions between the chains in the films. Since the strength of the van der Waals interactions per adsorbate is proportional to the number of methylene units in the adsorbate,[25a] films with longer methylene spacers form more highly stabilized interchain networks. This phenomenon correlates with the conformational order of the methylene spacers determined by PM-IRRAS (vide supra). Since film degradation involves the disruption of these networks, it readily follows that the presence of longer methylene moieties in semifluorinated SAMs imparts a greater stability against thermal degradation.

A previous report found that the length of the perfluorocarbon segment in semifluorinated alkanethiols influenced the thermal stability of the SAMs in contact with organic solvents.[33b] Given these results, we wished to evaluate the contribution of the length of the perfluorocarbon segments to the thermal stability of the SAMs under atmospheric conditions. To briefly explore this issue, we generated additional semifluorinated SAMs from F8H6SH and F13H17SH and compared their thermal stabilities to SAMs derived from F10H6SH and F10H17SH, respectively. Figure 7 shows the hexadecane contact angles of the monolayers as a function of incubation temperature. When the length of the methylene spacer is held constant at $n = 6$, final incubation at 180 °C revealed that the contact angle of the F8H6SH SAM decreased from 67 to 18° (73% decrease), while the contact angle of the F10H6SH SAM decreased from ∼70 to 25° (64% decrease). These data therefore suggest that the addition of two perfluoromethylene units affords a small enhancement in stability. This effect is amplified when the length of the methylene spacer is held constant at $n = 17$. After final incubation at 180 °C, the contact angles of the F13H17SH SAM decreased from 75 to 46° (39% decrease), while the contact angle of the F10H17SH SAM decreased from ∼70 to 25° (64% decrease). Both comparisons suggest that the thermal stability

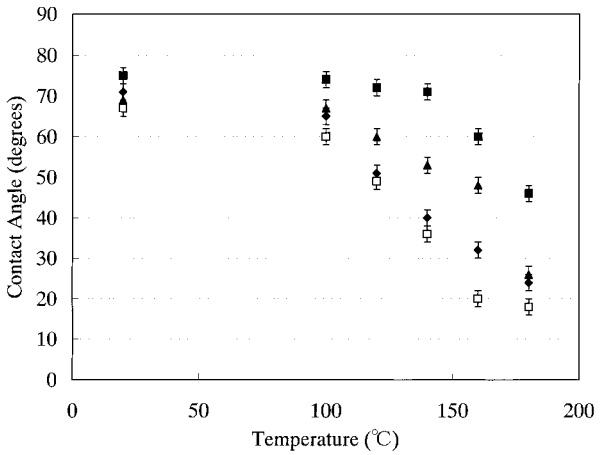

Figure 7. Plot of advancing contact angle vs incubation temperature. SAMs were generated from FmH*n*SH on Au/Ti/quartz substrates (□ = F8H6SH; ◆ = F10H6SH; ▲ = F10H17SH; ■ = F13H17SH).

of the semifluorinated SAMs increases as the length of the perfluorocarbon moiety increases.

The stabilization gained by increasing the number of perfluoromethylene units parallels the increase in melting points observed for semifluorinated *n*-alkanes $F(CF_2)_m(CH_2)_nH$ (F*m*H*n*), which, in accord with their structures, exhibit melting points higher than *n*-alkanes but lower than perfluoroalkanes.[34] Moreover, the increase in melting point is greater per additional perfluoromethylene than per additional methylene. Assuming that the initial steps of the thermal degradation of SAMs can be viewed as a "melting" of the crystalline chains to form liquidlike films, SAMs derived from F13H17SH would be expected to "melt" or disorder at a higher temperature than SAMs derived from F10H17SH. While this type of "melting" transition might serve as a prelude to film degradation, a direct correlation between these events is clouded by uncertainties involving the products and mechanism of the decomposition of SAMs on gold.[7a,25a,33] Nevertheless, it appears that longer fluorocarbon segments provide enhanced thermal stability, particularly when coupled with methylene spacers of sufficient length and conformational order (i.e., Hn > 10).

The overall picture of the degradation process still remain to be clarified. This will be the subject of further experimental and theoretical studies which are already being undertaken.

Conclusions

Semifluorinated SAMs generated by the adsorption of $F(CF_2)_{10}(CH_2)_nSH$, where $n = 2$, 6, 11, 17, and 33 (F10HnSH), onto the surface of gold were characterized by PM-IRRAS and dynamic contact angle measurements. These studies revealed that the length of the methylene spacer influenced the microstructure of the SAMs, which in turn influenced their wettability and thermal stability. The PM-IRRAS measurements showed that the terminal perfluorocarbon moiety became more tilted with respect to the surface normal as the length of the methylene segment increased. Furthermore, the conformational order of the methylene segment increased as its length increased. All of the semifluorinated SAMs exhibited low wettabilities toward water and hexadecane. However, the contact angles of hexadecane on SAMs derived from F10H2SH and F10H33SH were consistently lower than those of the other SAMs. The increased wettability of the F10H33SH SAM was attributed to increased surface disorder arising from the increased tilt of the fluorocarbon moiety. In contrast, the increased wettability of the F10H2SH SAM was attributed to either macroscopic surface roughness or the influence of lateral forces which are derived from attractive vdW interactions and repulsive dipole−dipole interactions. The thermal stability of the F10HnSH SAMs in air increased as the length of the methylene segment increased. The influence of the length of the fluorocarbon moiety was investigated by comparing SAMs derived from F8H6SH and F10H6SH as well as SAMs derived from F13H17SH and F10H17SH. Both comparisons showed that the thermal stability increased as the length of the perfluoromethylene segment increased. Taken together, these observations demonstrate that the wettability and thermal stability of semifluorinated alkanethiol films can be tailored by adjusting the lengths of the fluorocarbon and hydrocarbon segments.

Acknowledgment. The authors wish to thank Professors Colin Bain (Oxford University) and Nick Abbott (University of Wisconsin) for helpful discussions. We also thank Mr. Yoshiyuki Isobe (Seiko Epson Corp.) for assistance with the thermal stability characterization. The work at the University of Houston was supported by Seiko Epson Corp. and the National Science Foundation (Grant DMR-9700662).

References and Notes

(1) (a) Bain, C. D.; Whitesides, G. M. *J. Am. Chem. Soc*. **1988**, *110*, 5897. (b) Bain, C. D.; Troughton, E. B.; Tao, Y.-T.; Evall, J.; Whitesides, G. M.; Nuzzo, R. G. *J. Am. Chem. Soc*. **1989**, *111*, 321. (c) Evans, S. D.; Urankar, E.; Ulman, A.; Ferris, N. *J. Am. Chem. Soc*. **1989**, *113*, 4121. (d) Chidsey, C. E. D.; Loiacono, D. N. *Langmuir* **1990**, *6*, 682.

(2) (a) Häussling, L.; Michel, B.; Ringsdorf, H.; Rocher, H. *Angew. Chem., Int. Ed. Engl*. **1991**, *30*, 569. (b) Häussling, L.; Ringsdorf, H.; Schmitt, F.-J.; Knoll, W. *Langmuir* **1991**, *7*, 1837. (c) Spinke, J.; Liley, M.; Guder, H.-J.; Angermaier, L. *Langmuir* **1993**, *9*, 1821. (d) Nuller, W.; Ringsdorf, H.; Rump, E.; Wildburg, G.; Zhang, X.; Angermaier, L.; Knoll, W.; Liley, M.; Spinke, J. *Science* **1993**, *262*, 1706. (e) Prime, K. L.; Whitesides, G. M. *Science* **1991**, *252*, 1164.

(3) (a) Wolf, H.; Ringsdorf, H.; Delamarche, E.; Takami, T.; Kang, H.; Michel, B.; Gerber, Ch.; Jaschke, M.; Butt, H.-J.; Bamberg, E. *J. Phys. Chem*. **1995**, *99*, 7102. (b) Caldwell, W. R.; Campbell, D. J.; Chen, R.; Herr, B. R.; Mirkin, C. A.; Malik, A.; Durbin, M. K.; Dutta, P.; Huang, K. G. *J. Am. Chem. Soc*. **1995**, *117*, 6071. (c) Wang, R.; Iyoda, T.; Jing, L.; Hashimoto, K.; Fujishima, A. *Chem. Lett*. **1998**, 1005. (d) Roscoe, S. B.; Kakkar, A. K.; Marks, T. J.; Malik, A.; Durbin, M. K.; Lin, W.; Wong, G. K.; Dutta, P. *Langmuir* **1996**, *12*, 4218. (e) Kim, E., Whitesides, G. M.; Lee, L. K.; Smith, S. P.; Prentiss, M. *Adv. Mater*. **1996**, *8*, 139.

(4) (a) Drawhorn, R. A.; Abbott, N. L. *J. Phys. Chem*. **1995**, *99*, 16511. (b) Gupta, V. K.; Abbott, N. L. *Phys. Rev*. **1996**, *54*, 4540. (c) Gupta, V. K.; Abbott, N. L. *Science* **1996**, *273*, 885. (d) Miller, W. J.; Gupta, V. K.; Abbott, N. L.; Tsao, M. W.; Rabolt, J. F. *Liquid Cryst*. **1997**, *23*, 175. (e) Gupta, V. K.; Skaife, J. J.; Dubrovsky, T. B.; Abbott, N. L. *Science* **1998**, *279*, 2077.

(5) (a) Sondag-Huethorst, J. A. M.; van Helleputte, H. R. J.; Fokkink, L. G. J. *Appl. Phys. Lett*. **1994**, *64*, 285. (b) Huang, J.; Hemminger, J. C. *J. Am. Chem. Soc*. **1993**, *115*, 3342. (c) Hung, J.; Dahlgren, D. A.; Hemminger, J. C. *Langmuir* **1994**, *10*, 626. (d) Kumar, A.; Biebuyck, H. A.; Whitesides, G. M. *Langmuir* **1994**, *10*, 1498. (e) Kim, E.; Kumar, A.; Whitesides, G. M. *J. Electrochem. Soc*. **1995**, *142*, 628. (f) Rogers. J. A.; Jackman, R. J.; Whitesides, G. M. *Adv. Mater*. **1997**, *9*, 475.

(6) Green, J.-B. D.; MacDermott, M. T.; Porter, M. D. *J. Phys. Chem*. **1995**, *99*, 10960 and references contained therein.

(7) (a) Bensebaa, F.; Ellis, T. H.; Badia, A.; Lennox, R. B. *Langmuir* **1998**, *14*, 2361. (b) Bhatia, R.; Garrison, B. J. *Langmuir* **1997**, *13*, 765.

(8) (a) Batchelder, P. N.; Evans, S. D.; Freeman, T. L.; Haussling, L.; Ringsdorf, H. *J. Am. Chem. Soc*. **1994**, *116*, 1050. (b) Kim, T.; Qi, Y.; Li, S.; Chan, K. C.; Crooks, R. M. *Langmuir* **1996**, *12*, 6065. (c) Kim, T.; Chan, K. C.; Crooks, R. M. *J. Am. Chem. Soc*. **1997**, *119*, 189. (d) Mowery, M. D.; Evans, C. E. *J. Phys. Chem*. **1997**, *101*, 8513.

(9) Clegg, R. S.; Reed, S. M.; Hutchison, J. E. *J. Am. Chem. Soc*. **1996**, *118*, 2486.

(10) (a) Jennings, G. K.; Laibinis, P. E. *Langmuir* **1996**, *12*, 6137. (b) Jennings, G. K.; Laibinis, P. E. *J. Am. Chem. Soc*. **1997**, *119*, 5208.

(11) Alves, C. A.; Porter, M. D. *Langmuir* **1993**, *9*, 3507.

(12) Liu, G.; Fenter, P.; Chidsey, C. E. D.; Ogletree, D. F.; Eisenberger, P.; Salmeron, M. *J. Chem. Phys*. **1994**, *101*, 4301.

(13) (a) Garbassi, F.; Morroca, M.; Occhiello, E. *Polymer Surfaces*; Wiley: Chichester, U.K., 1994. (b) Kinloch, A. J. *Adhesion and Adhesives*; Chapman and Hall: New York, 1987. (c) Wu, S. *Polymer Interface and*

Adhesion; Marcel Dekker: New York, 1982. (d) Cosmacini, E.; Veronesi, V. *Wear* **1986**, *108*, 269. (e) Tsai, H.-C.; Mehmandoust, Y.; Samani, H.; Eltoukhy, A. *J. Vac. Sci. Technol. A* **1989**, *7*, 2491.

(14) Tsao, M.-W., Hoffmann, C. L.; Rabolt, J. F.; Johnson, H. E.; Castner, D. G.; Erdelen, C.; Ringsdorf, H. *Langmuir* **1997**, *13*, 4317.

(15) Lenk, T. J.; Hallmaek, V. M.; Hoffman, C. L.; Rabolt, J. F.; Castner, D. G.; Erdelen, C., Ringsdorf, H. *Langmuir* **1994**, *10*, 4610.

(16) (a) Schonherr, H.; Ringsdorf, H. *Langmuir* **1996**, *12*, 3891. (b) Schonherr, H.; Ringsdorf; Jaschke, M.; Butt, H.-J.; Banberg, E.; Allinson, H.; Evans, S. D. *Langmuir* **1996**, *12*, 3898. (c) Schonherr, H.; Vancso, G. J. *Langmuir* **1997**, *13*, 3769. (d) Ishida, T.; Yamamoto, S.; Mizutani, W.; Motomatsu, M.; Tokumoto, H.; Hokari, H.; Azehara, H.; Fujihira, M. *Langmuir* **1997**, *13*, 3261. (e) Ishida, T.; Yamamoto, S.; Mizutani, W.; Motomatsu, M.; Tokumoto, H.; Hokari, H.; Azehara, H.; Fujihira, M.; Kojima, I. *Jpn. J. Appl. Phys*. **1997**, *36*, 3909.

(17) Tamada, K.; Nagasawa, J.; Nakanishi, F.; Abe, K.; Hara, M.; Knoll, W.; Ishida, T.; Fukushima, H.; Miyashita, S.; Usui, T.; Koini, T.; Lee, T. R. *Thin Solid Films* **1998**, *327*, 150.

(18) Graupe, M.; Koini, T.; Wang, V. Y.; Nassif, G. M.; Colorado, R., Jr.; Villazana, R. J.; Miura, Y. F.; Shmakova, O. E.; Lee, T. R. *J. Fluorine Chem*. **1999**, *93*, 107.

(19) (a) Frey, S.; Heister, K.; Zharnikov, M.; Grunze, M.; Tamada, K.; Colorado, R., Jr.; Graupe, M.; Shmakova, O. E.; Lee, T. R. *Israel J. Chem.*, in press. (b) Colorado, R., Jr.; Shmakova, O. E.; Graupe, M.; Lee, T. R. Manuscript in preparation.

(20) Abe, K.; Takiguchi, H.; Tamada, K. *Langmuir* **2000**, *16*, 2394.

(21) Naselli, C.; Swalen, J. D.; Rabolt, J. F. *J. Chem. Phys*. **1989**, *90*, 3855.

(22) (a) Masetti, G.; Cabassi, F.; Moreli, G.; Zerbi, G. *Macromolecules* **1973**, *6*, 700. (b) Vanni, H.; Rabolt, J. F. *J. Polym. Sci., Polym. Phys. Ed*. **1980**, *18*, 587. (c) Rabolt, J. F.; Russell, T. P.; Twieg, R. J. *Macromolecules* **1984**, *17*, 3855.

(23) (a) Porter, M. D.; Bright, T. B.; Allara, D. L.; Chidsey, C. E. D. *J. Am. Chem. Soc*. **1987**, *109*, 3559. (b) Nuzzo, R. G.; Dubois, L. H.; Allara, D. L. *J. Am. Chem. Soc*. **1990**, *112*, 558. (c) Dubois, L. H.; Zegarski, B. R.; Nuzzo, R. G. *J. Electon Spectrosc. Relat. Phenom*. **1990**, *54*/*55*, 1143.

(24) Tamada, K.; Hara, M.; Sasabe, H.; Knoll, W. *Langmuir* **1997**, *13*, 1558.

(25) (a) Ulman, A. *An Introduction to Ultrathin Organic Films*; Academic: Boston, MA, 1991. (b) Bain, C. D.; Evall, J.; Whitesides, G. M. *J. Am. Chem. Soc*. **1989**, *111*, 7155. (c) Dubois, L. H.; Zegarski, B. R.; Nuzzo, R. G. *J. Am. Chem. Soc*. **1990**, *112*, 570.

(26) Miura, Y. F.; Takenaga, M.; Koini, T.; Graupe, M.; Garg, N.; Graham, R. L., Jr.; Lee, T. R. *Langmuir* **1998**, *14*, 5821.

(27) Tillman, N.; Ulman, A.; Schildkraut, J. S.; Penner, T. L. *J. Am. Chem. Soc*. **1988**, *110*, 6136.

(28) Chaudhury, M. K. *Mater. Sci. Eng*. **1996**, *R16*, 97.

(29) Characterization of these semifluorinated SAMs by AFM showed an average spacing of 5.9 Å: Tamada, K.; et al. Manuscript in preparation.

(30) Miller, W. J.; Abbott, N. L. *Langmuir* **1997**, *13*, 7106.

(31) Israelachvili, J. *Intermolecular & Surface Forces*; Academic: San Diego, CA, 1991.

(32) Graupe, M.; Takenaga, M.; Koini, T.; Colorado, R., Jr.; Lee, T. R. *J. Am. Chem. Soc*. **1999**, *121*, 3222.

(33) (a) Evans, S. D.; Urankar, E.; Ulman, A.; Ferris, N. *J. Am. Chem. Soc*. **1991**, *113*, 4121. (b) Shmakova, O. E.; Colorado, R., Jr.; Graupe, M.; Lee, T. R. *Abstr. Pap.—Am. Chem. Soc*. **1998**, COLL 192. (c) Schoenfisch, M. H.; Pemberton, J. E. *J. Am. Chem. Soc*. **1998**, *120*, 4502.

(34) Rabolt, J. F.; Russell, T. P.; Twieg, R. J. *Macromolecules* **1984**, *17*, 2786.